

Multiferroicity in the frustrated spinel cuprate  $\text{GeCu}_2\text{O}_4$ 

L. Zhao, L. Muzica, U. Schwarz, and A. C. Komarek\*

*Max Planck Institute for Chemical Physics of Solids, Nöthnitzer Str. 40, 01187 Dresden, Germany* (Received 21 November 2017; revised manuscript received 19 March 2018; published 24 April 2018)

Different from other magnetically frustrated spinel systems,  $\text{GeCu}_2\text{O}_4$  is a strongly tetragonal distorted spinel cuprate in which edge-sharing  $\text{CuO}_2$  ribbons are running along alternating directions perpendicular to the  $c$  axis. Here,  $\text{GeCu}_2\text{O}_4$  samples of high quality were prepared via high-pressure synthesis (at 4 GPa) and the corresponding magnetic and dielectric properties were investigated. We observed a ferroelectric polarization emerging at  $T_N \sim 33$  K. Although the ferroelectric polarization is weak in  $\text{GeCu}_2\text{O}_4$  ( $P \sim 0.2 \mu\text{C}/\text{m}^2$ ), the existence of spin-induced multiferroicity provides a strong constraint on the possible ground-state magnetic structures and/or the corresponding theoretical models of multiferroicity for  $\text{GeCu}_2\text{O}_4$ .

DOI: [10.1103/PhysRevMaterials.2.041402](https://doi.org/10.1103/PhysRevMaterials.2.041402)

Low-dimensional  $S = 1/2$  quantum spin systems have been a challenging topic of continued interest within contemporary condensed-matter physics. A vast amount of materials with atomic arrangements including quasi-two-dimensional (2D) layers based on square lattices, plaquettes, triangular or kagome lattices, quasi-one-dimensional (1D) spin chains, or ladders are known to exhibit a wide variety of fascinating quantum phenomena at low temperature [1] such as superconductivity, spin dimerization, Bose-Einstein condensation, quantum spin liquid states, and also multiferroicity which can be observed in these systems with competing charge, spin, orbital, and lattice degrees of freedom.

Transition-metal oxides with spinel structure have the general chemical formula  $AB_2O_4$ . These materials have been a playground for theoretical studies on frustrated quantum magnets. The  $B$  ions form a three-dimensional (3D) network of corner-sharing tetrahedra similar to a pyrochlore lattice which gives rise to strong geometrical frustration for antiferromagnetically coupled  $B$ -site spins. Theoretically, a quantum spin liquid ground state can be realized in the ideal isotropic pyrochlore lattice. It is well known that many spinel magnetic compounds exhibit unusual magnetic properties and various ground states with or without long-range magnetic ordering. The material-specific details like ion anisotropy and structural distortions are able to lift the high degeneracy [2].

$\text{GeCu}_2\text{O}_4$  crystallizes in a strongly distorted spinel structure (Hausmannite) with space group  $I4_1/amd$  [3]. The lattice parameters amount to  $a = b = 5.593 \text{ \AA}$  and  $c = 9.396 \text{ \AA}$ .  $\text{GeCu}_2\text{O}_4$  exhibits drastically elongated  $\text{CuO}_6$  octahedra in the  $c$  direction due to a strong Jahn-Teller effect for the  $\text{Cu}^{2+}$  ions [see Fig. 1(a)]. The  $ab$ -plane “intrachain” exchange  $J$  in the  $a$  or  $b$  direction is much larger than the “interchain” exchange  $J_x$  in the  $c$  direction. From the analysis of its magnetic susceptibility  $J_x/J \sim 0.16$  has been reported [4]. The interaction between chains in the same layer is also weak. The directions of these chains are orthogonal to those lying in the neighboring layers.

Theoretically the real pyrochlore lattice can be simplified by the projection onto a 2D checkerboard pattern known as the planar pyrochlore antiferromagnetic and crossed-chain model, which conserves the magnetic frustration and interaction anisotropy. In the simple anisotropic limit ( $J_x \ll J$ ) which might be assumed for  $\text{GeCu}_2\text{O}_4$  a crossed-dimer ground state is predicted [5]. Later, a more detailed work combined with density-functional calculations proposed the ground state of  $\text{GeCu}_2\text{O}_4$  being a spin spiral state along the chains of edge-sharing  $\text{CuO}_4$  plaquettes [6]. The spiral state is common for many quasi-1D frustrated  $J_1$ - $J_2$  spin chain compounds. Such a spiral magnetic structure is able to induce electric polarization and strong magnetoelectric coupling [7]. However, the calculation [6] predicts an opposite twisting direction for neighboring chains arising from the interchain exchange and, thus, no macroscopic polarization.

So far, only a few measurements have been reported on the physical properties of  $\text{GeCu}_2\text{O}_4$  [4,8] since the spinel is metastable and can only be synthesized at high pressure [3]. In spite of the three-dimensional nature of the spinel structure, a magnetic susceptibility characteristic for a quasi-1D Heisenberg spin-1/2 chain system with  $J$  of  $\sim 135$  K has been reported [4]. Moreover, long-range antiferromagnetic ordering emerges below 33 K. Very recently, a powder neutron diffraction experiment [8] reported a novel collinear “up-up-down-down” ( $\uparrow\uparrow\downarrow\downarrow$ ) pattern along each spin chain within the  $ab$  plane, which contradicts previous theoretical predictions [6]. However, also for the experimentally observed magnetic structure [8] no multiferroicity can be expected.

We noticed that the complex structure of  $\text{GeCu}_2\text{O}_4$  which consists of intertwined quasi-1D  $\text{CuO}_2$  spin chains strongly resembles some structural motifs in  $\text{CuO}_2\text{Cl}_2$  [9].  $\text{CuO}_2\text{Cl}_2$  is a newly discovered spin-driven multiferroic material [10] with high transition temperature ( $\sim 70$  K). Hence, we synthesized  $\text{GeCu}_2\text{O}_4$  single crystals at high pressures and analyzed the dielectric and pyroelectric properties of this spinel oxide. Our measurements reveal the unexpected existence of multiferroicity in  $\text{GeCu}_2\text{O}_4$  questioning the reported models of its magnetic ground state.

First, polycrystalline mixtures were prepared by solid-state reaction. The starting materials of  $\text{GeO}_2$  and  $\text{CuO}$  were mixed

\*Alexander.Komarek@cpfs.mpg.de

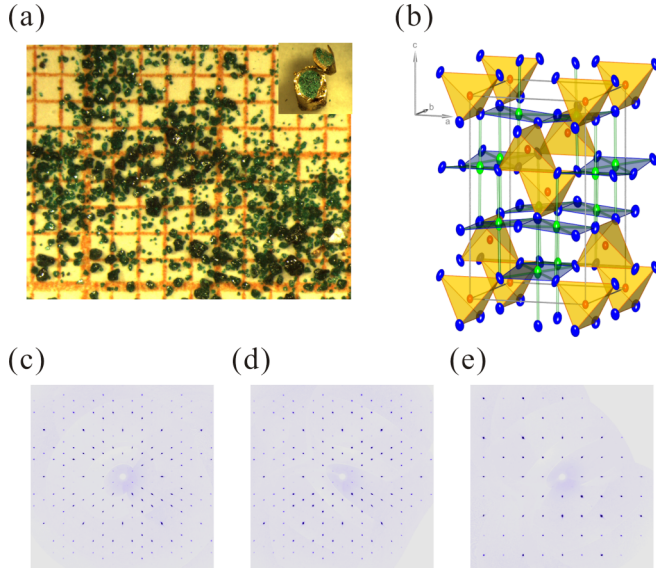


FIG. 1. (a) A photo of our synthesized  $\text{GeCu}_2\text{O}_4$  single crystals. (b) Representation of the crystal structure of  $\text{GeCu}_2\text{O}_4$  as obtained from our single-crystal x-ray diffraction measurement. The Cu-oxygen plaquettes are indicated by the blue areas; red, green, and blue ellipsoids denote Ge, Cu, and O ions, respectively (99% probability ellipsoids). (c)–(e) X-ray scattering intensities in the  $0KL$ ,  $H0L$ , and  $HK0$  planes of reciprocal space indicating the single-crystalline nature of our  $\text{GeCu}_2\text{O}_4$  single crystal.

in a molar ratio of 1:2 and then sintered for 50 h at  $850^\circ\text{C}$  in air with intermediate grindings. The resulting blue product is composed of  $\text{GeCuO}_3$  and  $\text{CuO}$  as confirmed by powder x-ray diffraction. Next, the obtained powder was sealed in cylindrical gold capsules, which were inserted in a BN sleeve and then pressurized with a multianvil high-pressure apparatus to 4 GPa pressure and, finally, heated to  $900^\circ\text{C}$ . After annealing at  $900^\circ\text{C}$  for 30 min, the sample was cooled to room temperature before the high pressure was released. Quasihydrostatic pressures were generated with a Walker-type multianvil assembly [11] in combination with a hydraulic press for force generation. For pressure redistribution, we used octahedra manufactured from  $\text{MgO}$  with 5%  $\text{Cr}_2\text{O}_3$  and an edge length of 18 mm. Calibration of  $p, T$  conditions was performed independently before the experiments. Temperatures were measured with type-C thermocouples and pressures were determined using the resistivity changes of Bi and Pb at room temperature. Within the gold capsule a dense green pillar could be obtained after the high-pressure synthesis. This color change from blue to green has also been observed in previous reports of the high-pressure synthesis of  $\text{GeCu}_2\text{O}_4$  [3]. If the dwelling time at  $900^\circ\text{C}$  was enhanced and the subsequent cooling rate was decreased, the aggregation of small transparent green single crystals (grown via self-nucleation) of 50 to  $500\ \mu\text{m}$  size could be observed [see Fig. 1(a)].

Powder x-ray diffraction (XRD) measurements have been performed using  $\text{Cu}\ K\alpha 1$  radiation on a Bruker D8 Discover A25 powder x-ray diffractometer indicating a single phase of  $\text{GeCu}_2\text{O}_4$ .

Single-crystal XRD measurements have been performed at room temperature using  $\text{Mo}\ K\alpha$  radiation on a Bruker D8VENTURE single-crystal x-ray diffractometer equipped

TABLE I. Structural parameters derived from the crystal structure refinement of our single-crystal x-ray diffraction measurement;  $a = 5.5929(4)\ \text{\AA}$ ,  $c = 9.3984(6)\ \text{\AA}$ ; space group:  $I4_1/amd$ .

Atom	$x$	$y$	$z$
Ge1	0	0	0
Cu1	0	1/4	5/8
O1	0	0.24171(9)	0.35882(6)
Atom	$U_{11}\ (\text{\AA}^2)$	$U_{22}\ (\text{\AA}^2)$	$U_{33}\ (\text{\AA}^2)$
Ge1	0.00196(3)	0.00196(3)	0.00389(5)
Cu1	0.00273(5)	0.00238(4)	0.00786(5)
O1	0.00367(16)	0.00306(16)	0.00725(15)
Atom	$U_{12}\ (\text{\AA}^2)$	$U_{13}\ (\text{\AA}^2)$	$U_{23}\ (\text{\AA}^2)$
Ge1	0	0	0
Cu1	0	0	0.00010(3)
O1	0	0	0.00184(11)
Atom	$U_{\text{iso}}\ (\text{\AA}^2)$	Occup.	
Ge1	0.00260(2)	1	
Cu1	0.00432(3)	1	
O1	0.00466(9)	1	

with a bent graphite monochromator for about  $3\times$  intensity enhancement and a Photon complementary metal-oxide semiconductor large-area detector. An as-grown single crystal with roughly  $40\text{-}\mu\text{m}$  diameter has been measured and a multiscan absorption correction has been applied to the data (minimum and maximum transmission: 0.5706 and 0.7536, respectively). For space group  $I4_1/amd$  17773 reflections ( $H: 13 \rightarrow 10$ ,  $K: 12 \rightarrow 14$ , and  $L: 21 \rightarrow 21$ ) have been collected with an internal  $R$  value of 2.71%, a redundancy of 24.0 and 99% (89.7%) coverage up to  $2\Theta = 117.7^\circ$  ( $144.5^\circ$ ). The goodness of fit, the  $R$  and weighted  $R$  values within the crystal structure refinement amount to 1.63%, 1.53%, and 4.27%, respectively. The structural parameters are listed in Table I and the obtained crystal structure is plotted in Fig. 1(b). The x-ray scattering intensities within different planes in reciprocal space are shown in Figs. 1(c)–1(e) and indicate the single-crystalline nature of our measured crystal.

For the study of the dielectric properties of  $\text{GeCu}_2\text{O}_4$ , the dense polycrystalline sample was cut and polished to thin plates with thickness of 0.1–0.3 mm. Silver paint was applied to both sides as electrodes to form parallel plate capacitors whose capacitance is proportional to the dielectric constant  $\epsilon$ . The samples have been mounted on the cryogenic stage and inserted in a Quantum Design 9T-PPMS. A high-precision capacitance bridge (AH 2700A; Andeen-Hagerling, Inc.) was used for dielectric measurements. No apparent difference was observed in the different measuring conditions (various excitation voltages, sweeping rates, and integration times have been applied). The electric polarization has been obtained by the pyroelectric current method. First, we polarized the specimens during the cooling process with a static electric field of 1–5 MV/m. Then, we short-circuited both sides of the sample at base temperature for about 1 h in order to remove any possible trapped interfacial charge carriers. The pyroelectric current was measured on heating with a heating rate of 3–5 K/min. The electric polarization  $P$  has been obtained from the integration of the measured pyroelectric

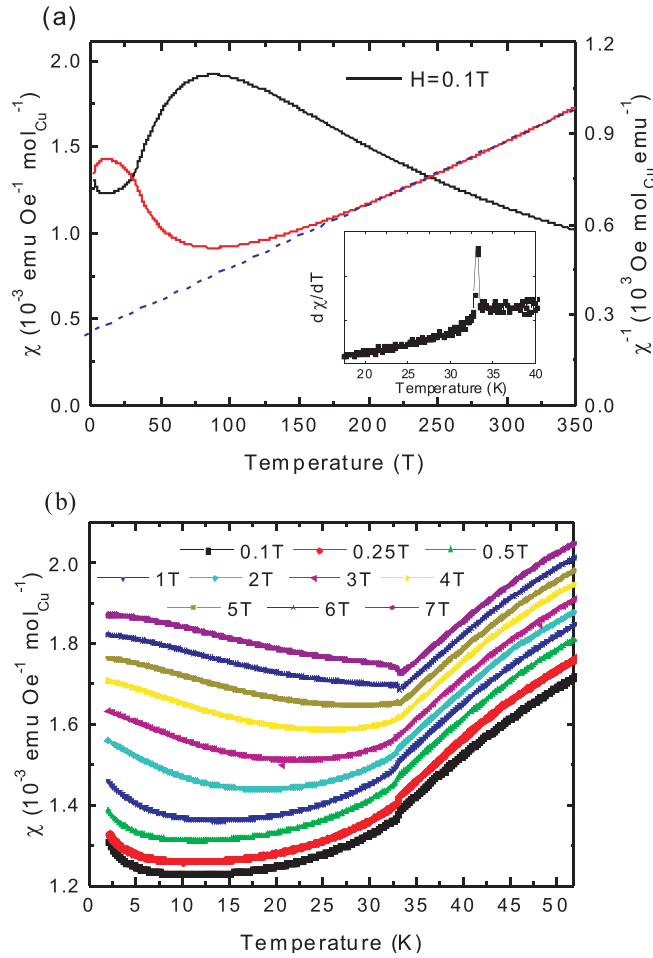


FIG. 2. (a) The temperature dependence of the magnetic susceptibility  $\chi(T)$  of  $\text{GeCu}_2\text{O}_4$  (black) and  $\chi^{-1}$  (red) measured in an external field  $H$  of 0.1 T. The dashed line denotes a Curie-Weiss fit. In the inset the derivative ( $d\chi/dT$ ) is shown. (b)  $\chi$  measured under different applied fields  $H$  ranging from 0.1 to 7 T. For clarity, all the curves are shifted vertically except for  $H = 0.1$  T.

current. Magnetic properties have been measured on a SQUID magnetometer (MPMS3; Quantum Design, Inc.).

The temperature dependence of the magnetic susceptibility  $\chi(T)$  of  $\text{GeCu}_2\text{O}_4$  measured in a field of 0.1 T is shown in Fig. 2(a). Zero-field-cooled and field-cooled measurements coincide. At around 80 K a broad hump appears which is characteristic for short-range antiferromagnetic ordering due to frustration effects. A simple Curie-Weiss fit within the temperature range of 180–350 K yields a Curie-Weiss temperature  $\theta_{CW}$  of about  $-110$  K and an effective magnetic moment  $\mu_{eff}$  which amounts to  $\sim 1.94\mu_B$  which is similar with previous studies [4]. The value of  $\mu_{eff}$  is slightly higher than what might be expected for the paramagnetic  $\text{Cu}^{2+}$  spin-only value ( $1.73\mu_B$ ). At low temperature  $\chi(T)$  exhibits a slight drop at  $T_N \sim 33$  K suggesting the emergence of long-range magnetic ordering. As shown in the inset, the corresponding temperature derivative exhibits a sharp peak at  $T_N$ .

We also studied the magnetic field dependence of  $\chi(T)$  for different fields up to 7 T. All  $\chi(T)$  curves coincide above  $T_N$  (including the value of  $T_N$ ). On cooling below  $T_N$ , the temper-

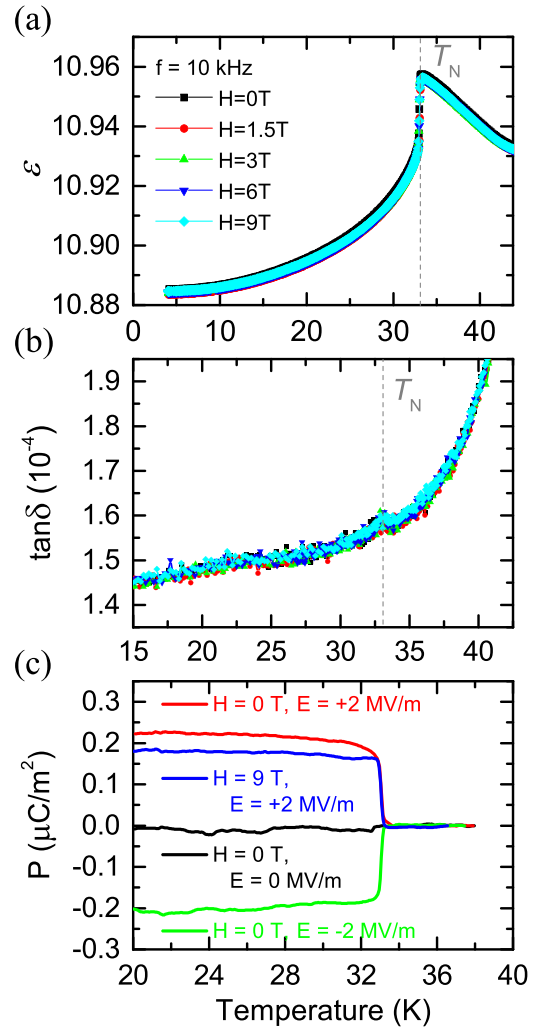


FIG. 3. Temperature dependence of the dielectric constant  $\epsilon(T)$  of polycrystalline  $\text{GeCu}_2\text{O}_4$  under different magnetic fields  $H = 0-9$  T. (b) The corresponding tangential loss  $\tan\delta$ . All these curves have been measured at the frequency of 10 kHz. (c) The temperature dependence of the electric polarization (obtained by integration of the pyroelectric current) which was measured after different poling processes (+2, 0, and  $-2$  MV/m).

ature dependence of  $\chi(T)$  changes from a decreasing behavior in low fields to an increasing one in high fields above 4 T.

Our results resemble those reported in Ref. [8] where  $\chi(T)$  was also explained by adding a minor contribution of paramagnetic impurities like  $\text{GeO}_2$ . In fact, about 3.6%  $\text{GeO}_2$  was found in their samples according to x-ray diffraction. However, no such impurities exist in our  $\text{GeCu}_2\text{O}_4$  samples. [We also measured the magnetic susceptibilities of pure  $\text{GeO}_2$ ,  $\text{GeCuO}_3$ , and  $\text{CuO}$  powder as reference materials in order to search for possible impurities below the detection level of x-ray diffraction. But, no anomalies could be detected around 33 K for these reference materials, thus, confirming that our observed field evolution of  $\chi(T)$  is intrinsic for  $\text{GeCu}_2\text{O}_4$ .]

The temperature dependence of the dielectric constant  $\epsilon(T)$  measured at a frequency of 10 kHz for different fields  $H$  is shown in Fig. 3(a). On cooling  $\epsilon$  slightly increases for temperatures somewhat above  $T_N$  and then  $\epsilon$  drops sharply

at the magnetic transition temperature  $T_N$ . In our experiments, we also measured  $\epsilon$  with various frequencies between 1 and 20 kHz (not shown here), and the observed dielectric anomaly shows no difference for all tested measuring frequencies. This confirms the intrinsic origin of the dielectric anomaly at  $T_N$  which—although weak—can also be seen in the corresponding dielectric loss [see Fig. 3(b)]. As shown in Figs. 3(a) and 3(b), the effect of external magnetic fields on the dielectric behavior is almost negligible for the whole studied range of magnetic fields  $H$  up to 9 T.

Moreover, we measured also the pyroelectric current in order to study the electric polarization of  $\text{GeCu}_2\text{O}_4$ . A small but sharp pyroelectric current peak emerges at  $T_N$ . The electric polarization in  $\text{GeCu}_2\text{O}_4$  was obtained by integrating the small pyroelectric currents with our high SNR (signal-to-noise ratio) setup [see Fig. 3(c)]. To minimize the accumulative error and uncertainty due to noise within the background, the integration was carried out from above  $T_N$  to just above 20 K where the polarization has almost saturated ( $P_s$  in our notion). Although  $P_s$  is quite small—about  $0.2 \mu\text{C}/\text{m}^2$  at 20 K—it can be inverted with opposite poling, whereas the measured pyroelectric current and corresponding polarization is negligible for zero poling field [see Fig. 3(c)]. Our observation reveals the weak ferroelectric nature of  $\text{GeCu}_2\text{O}_4$  below  $T_N$ . In  $\text{GeCu}_2\text{O}_4$ , the polarization and magnetoelectric effect is much weaker than in most known multiferroic cuprates such as  $\text{LiCu}_2\text{O}_2$  [16]. However, we discovered a multiferroic material with a strongly tetragonally distorted spinel structure.

The appearance of a ferroelectric polarization below the magnetic ordering temperature is indicative for spin-induced multiferroicity in  $\text{GeCu}_2\text{O}_4$ . The appearance of an electric polarization that is induced by the magnetic structure has been studied thoroughly in recent years [12–14]. Three major microscopic origins of spin-induced ferroelectricity are known. (i) Exchange striction arising from the symmetric spin-exchange interaction in certain collinear spin ordering states in some frustrated systems with magnetically inequivalent ions. The up-up-down-down spin arrangement along the atomically alternating  $A$ - $B$  spin chains observed in  $\text{Ca}_3(\text{Co},\text{Mn})\text{O}_6$  [15] is an example for this first mechanism. (ii) The inverse Dzyaloshinskii-Moriya or spin current model. Via spin-orbit interaction two noncollinear magnetic moments are able to induce a local electric polarization  $\mathbf{P}_{ij} = A\hat{\mathbf{e}}_{ij} \times (\mathbf{S}_i \times \mathbf{S}_j)$  with  $\hat{\mathbf{e}}_{ij}$  being the unit vector between the two sites  $i$  and  $j$ . (iii) The Arima model where the spin-dependent  $p$ - $d$  hybridization induces a local polarization  $P_{il} \propto (S_i \cdot \hat{\mathbf{e}}_{il})^2 \hat{\mathbf{e}}_{il}$  with  $\hat{\mathbf{e}}_{il}$  being

the unit vector connecting the magnetic ion and the ligand site. The last two models (ii) and (iii) require certain magnetic and/or lattice structures such that the sum over the crystal lattice sites is not canceled out and such that a nonzero macroscopic polarization  $P$  emerges. Model (ii) is able to yield nonzero  $P$ , e.g., for cycloidal magnetic structures [16], whereas model (iii) requires a certain Bravais lattice that hosts, e.g., a screw-type helical magnetic structure [17]. For both models (ii) and (iii) the magnitude of the induced polarization  $P$  is usually rather weak.

In  $\text{GeCu}_2\text{O}_4$  the presence of identical magnetic ions, i.e.,  $\text{Cu}^{2+}$  ions, excludes the possibility of mechanism (i). The lattice symmetry (space group  $I4_1/amd$ ) also excludes the possibility of the last mechanism (iii). For the spiral magnetic ground state that was theoretically predicted [6] the spins are spiraling along each chain with the renormalized pitch angle of about  $84^\circ$ . But, the induced polarization cancels out due to opposite twisting directions in neighboring chains. Also for the cross-dimer state [5] no polarization  $P$  can be expected since this dimer ground state does not break inversion symmetry. For example,  $\text{GeCuO}_3$  is such a spin-dimer system where no dielectric anomaly could be observed at  $T_N$  [18]. So far, there is only one reported neutron diffraction measurement on a  $\text{GeCu}_2\text{O}_4$  powder sample [8]. The experimentally measured collinear up-up-down-down spin structure is also centrosymmetric and incompatible with the emergence of spin-induced multiferroicity. Hence, further studies on its spin structure based on high-quality powder samples or single crystals would be desirable for an understanding of the mechanism of multiferroicity in  $\text{GeCu}_2\text{O}_4$ .

Conclusively, in this work, we presented magnetic, dielectric, and polarization measurements on the metastable  $\text{GeCu}_2\text{O}_4$  spinel oxide prepared by high-pressure synthesis. We observed spin-induced ferroelectricity in  $\text{GeCu}_2\text{O}_4$ , where all the experimentally or theoretically proposed spin structures are not compatible with existing theoretical models for multiferroicity (or vice versa). Due to the complex intertwining of quasi-1D  $\text{CuO}_2$  spin chains and strong inherent frustration effects within the tetragonally distorted spinel structure, interesting physics can be expected as an outcome of future theoretical and experimental studies on this multiferroic material.

We would like to thank R. Castillo for support in the sample preparation. We also would like to thank L. H. Tjeng for his support and for helpful discussions. The research is partially supported by the Deutsche Forschungsgemeinschaft through SFB 1143 and through DFG Project No. 320571839.

- 
- [1] U. Schollwöck, J. Richter, D. J. J. Farnell, and R. F. Bishop, *Quantum Magnetism* (Springer, New York, 2004).
- [2] H. Takagi and S. Niitaka, *Introduction to Frustrated Magnetism* (Springer, New York, 2010), Chap. 7, p. 155.
- [3] W. Hegenbart, F. Rau, and K.-J. Range, *Mater. Res. Bull.* **16**, 413 (1981).
- [4] T. Yamada, Z. Hiroi, M. Takano, M. Nohara, and H. Takagi, *J. Phys. Soc. Jpn.* **69**, 1477 (2000).
- [5] O. A. Starykh, A. Furusaki, and L. Balents, *Phys. Rev. B* **72**, 094416 (2005).
- [6] A. A. Tsirlin, R. Zinke, J. Richter, and H. Rosner, *Phys. Rev. B* **83**, 104415 (2011).
- [7] Y. Tokura and S. Seki, *Adv. Mater.* **22**, 1554 (2010).
- [8] T. Zou, Y.-Q. Cai, C. R. dela Cruz, V. O. Garlea, S. D. Mahanti, J.-G. Cheng, and X. Ke, *Phys. Rev. B* **94**, 214406 (2016).
- [9] S. V. Krivovichev, S. K. Filatov, and P. C. Burns, *Can. Mineral.* **40**, 1185 (2002).
- [10] L. Zhao, M. T. Fernández-Díaz, L. H. Tjeng, and A. C. Komarek, *Sci. Adv.* **2**, e1600353 (2016).

- [11] D. Walker, M. A. Carpenter, and C. M. Hitch, *Am. Mineral.* **75**, 1020 (1990).
- [12] S.-W. Cheong and M. Mostovoy, *Nat. Mater.* **6**, 13 (2007).
- [13] Y. Tokura, S. Seki, and N. Nagaosa, *Rep. Prog. Phys.* **77**, 076501 (2014).
- [14] K. F. Wang, J.-M. Liu, and Z. F. Ren, *Adv. Phys.* **58**, 321 (2009).
- [15] Y. J. Choi, H. T. Yi, S. Lee, Q. Huang, V. Kiryukhin, and S.-W. Cheong, *Phys. Rev. Lett.* **100**, 047601 (2008).
- [16] S. Park, Y. J. Choi, C. L. Zhang, and S.-W. Cheong, *Phys. Rev. Lett.* **98**, 057601 (2007).
- [17] T. Arima, *J. Phys. Soc. Jpn.* **76**, 073702 (2007).
- [18] Y. Tsunazumi, N. Ogita, J. Akimitsu, E. Nakamura, and M. Udagawa, *J. Phys. Soc. Jpn.* **65**, 3404 (1996).